Introduction to Diffractive Photoprocesses

Graham Shaw*

Department of Physics and Astronomy, University of Manchester, Manchester M13 9PL, U.K.

Abstract. The objectives of my talk are to provide a very brief introduction to diffractive photoprocesses in general and the colour dipole model in particular; and to comment on possible gluon saturation effects at HERA and beyond.

INTRODUCTION

Diffraction exchange is the study of vacuum exchange at high energies. It is frequently divided into elastic, singly-dissociative and double dissociative processes as illustrated in Figure 1, where A and B may be photons or hadrons and X and Y may be single particles or an inclusive sum over $n \geq 1$ particle states. The wiggly line indicates an

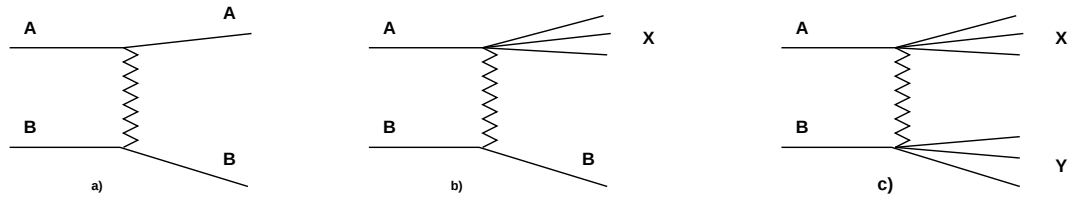

FIGURE 1. (a) elastic (b) singly dissociative and (c) double dissociative diffractive processes. (Figure from [1]).

exchange of energy and momentum, but no non-zero colour or flavour quantum numbers may be exchanged. High energy means that the square of the centre of mass energy $s = W^2$ is much larger than any other energy scale:

$$s \gg t, m_X^2, \ldots \quad .$$

For diffractive processes initiated by virtual photons, the latter include the virtuality Q^2, implying

$$x = Q^2/s \ll 1 \quad .$$

We note that t, m_X^2, Q^2 can themselves become large, provided they remain much smaller than s.

Experimentally, diffractive processes are characterized by two distinctive features: **rising cross-sections** and **rapidity gaps**. The two groups of final state particles in Figure 1 emerge in roughly the forward and backward directions in the centre of mass frame; and are well-separated in rapidity or pseudo-rapidity

$$\eta = -\ln\tan(\frac{\theta}{2})$$

where θ is the polar angle with respect to the beam direction. Such rapidity gaps are characteristic of colour singlet exchange, in contrast to the hadronization strings associated with colour exchange. They occur not only in diffractive processes, but in, for example, colour singlet meson exchange processes. However meson exchange gives rise to cross-sections which fall rapidly with increasing energy, in contrast to diffractive processes which have constant or rising cross-sections. Nonetheless at finite energies one may need to take account of small contributions from the exchange of flavour singlet meson exchange contributions, which can in general interfere with the dominant diffractive process.

Diffractive processes, so defined, are copious and varied. For example the singly dissociative inclusive reaction

$$\gamma^* + p \to X + p \ , \tag{1}$$

where X is an inclusive sum over hadronic states, accounts for 10-20 % of the $\gamma^* p$ total cross-sections at low x. (Here and throughout, γ^* indicates either a real or virtual photon, while γ refers exclusively to real photons.) This reaction has stimulated an enormous literature already [2] and new data will be presented here [3]. Of particular interest is the behaviour for $M_X^2 \gg Q^2$, which explores aspects of diffraction which are not easily studied in other processes. Exclusive processes discussed at the conference include: elastic virtual Compton scattering

$$\gamma^* + p \to \gamma^* + p \ ,$$

which is not measured directly, but is related to the $\gamma^* p$ total cross-sections and hence the deep inelastic structure functions via the optical theorem; deeply virtual Compton scattering(DVCS)

$$\gamma^* + p \to \gamma + p \ , \tag{2}$$

for which the first data are presented at this conference [4]; and the vector meson production processes [5]

$$\gamma^* + p \to \rho + p \tag{3}$$

$$\gamma^* + p \to J/\Psi + p \tag{4}$$

where measuring the vector meson decay products the enables the spin structure of the interaction and the separate contributions from longtitudinal and transverse photons to be studied. In addition, the J/ψ mass introduces an at least moderately large scale into the problem even for real photons. Perturbative aspects of diffraction can also be enhanced by working at high t [6] and/or by the study of diffractive jet production [7]. Finally some of the first results on diffraction in $\gamma^*\gamma^*$ collisions are also reported [8].

THEORETICAL FRAMEWORK

Diffraction involves an interplay of perturbative and non-perturbative effects which presently defies a rigorous treatment in QCD. Rather there are innumerable models which throw light on different aspects of the problem with varying degrees of success. Here we try to provide a simple framework which can be used to classify and compare the various models and hopefully avoid confusion. To do this we emphasize two features.

Vacuum exchange.

The first thing to consider is the way the model implements vacuum exchange. There are three main approaches, which we will list for the moment and illustrate later.

- **Regge models**, in which the vacuum exchange is usually described by the exchange of one or more Regge poles with vacuum quantum numbers, called pomerons.
- **Gluon exchange models** in which the vacuum exchange is modelled by the exchange of two or more gluons in a colour singlet state.
- **Quasi-optical models** in which the projectile is regarded as a superposition of "scattering eigenstates" which are either absorbed or scatter unchanged at fixed impact parameter on traversing the "target."

Reference frames

Different reference frames are conveniently chosen to emphasize different aspects of the physics and caution is required in comparing dynamical models formulated in different frames. Popular choices for discussing $\gamma^* p$ collisions include:

- The **infinite momentum frame** in which, for large Q^2 at least, the parton distribution functions(pdfs) have a simple interpretation and the photon is regarded as pointlike.
- The **laboratory frame** in which the incoming photon is typically absorbed a long distance, of order $1/(Mx)$ from the proton target and the intermediate states into which it converts are usually regarded as constituents of the photon.

HARD AND SOFT DIFFRACTION

The study of diffraction has been transformed by the discovery of hard diffraction in $\gamma^* p$ collisions at HERA. Here we summarize this discovery and some of the questions it raises.

Diffraction in hadron physics

Before discussing diffractive photoprocesses, it is useful to comment on the "soft diffraction" observed in purely hadronic processes. At high energies $s \gg t$, hadronic scattering is well-described by Regge pole exchange, as illustrated in Figure 2 for the charge exchange reaction $\pi^- p \to \pi^0 n$. If a single pole i dominates, the differential

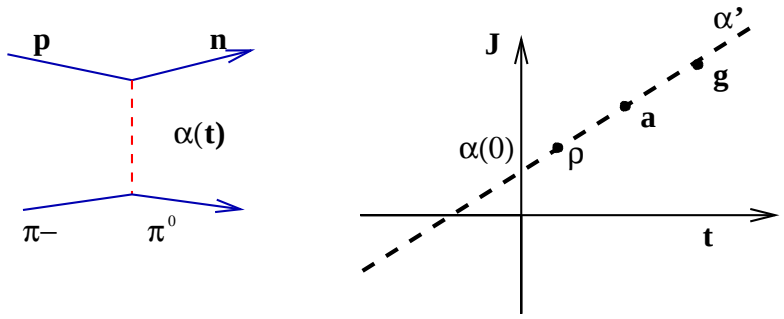

FIGURE 2. Regge pole exchange for the reaction $\pi^- p \to \pi^0 n$ and the associated meson trajectory (7)(Figure from [9]) .

cross-section for any $2 \to 2$ reaction satisfies

$$\frac{d\sigma}{dt} \propto \left(\frac{s}{s_0}\right)^{2\alpha_i(t)-2} , \tag{5}$$

where s_0 is a convenient scale, usually taken to be 1 GeV^{-2}, and the *Regge trajectories*

$$\alpha_i(t) = \alpha_i(0) + \alpha_i' t \tag{6}$$

are found to be approximately linear. They relate the observed energy dependence in the scattering region $t \leq 0$ to the exchanged mesons at $\alpha(t = m_j^2) = j$, where j, m_j^2 are the spin and mass of the meson respectively. The picture applies to baryon as well as meson exchange, with an approximately universal *slope parameter* $\alpha' \approx 1$ GeV^{-2}. In contrast the *intercept* $\alpha_i(0)$ depends on the flavour exchange quantum numbers i, with

$$\alpha_M(t) \approx 0.5 + t \tag{7}$$

for the leading non-strange meson trajectories, leading to cross-sections (5) which fall roughly like $1/s$.

The above picture accounts remarkably well for reactions with non-zero flavour exchange, including other features - shrinkage, factorisation, dips - not mentioned here. It can be extended successfully to vacuum exchange processes by adding a single additional Regge pole to describe diffraction, called the pomeron. Specifically the available data on a wide range of different reactions is consistent with the same universal trajectory [10]

$$\alpha_P(t) \approx 1.08 + 0.25t \ . \tag{8}$$

where the high value of the intercept $\alpha_P(0)$ reflects the fact that diffractive cross-sections rise slowly with energy. In addition, the pomeron slope $\alpha_P' \approx 0.25$ GeV^{-2} differs markedly from the approximately universal slope $\alpha_P' \approx 1$ observed for all $q\bar{q}$ meson and qqq baryon Regge poles, suggesting the pomeron is not associated with $q\bar{q}$ meson exchange. It is rather assumed to be associated with the exchange of gluons, so that particles lying on the pomeron trajectory are presumably glueballs. The lightest glueball on the trajectory (8) is a 2^+ particle with a predicted mass of around 1.9 GeV. This is not unreasonable, although it must be said that little is known from experiment about the glueball spectrum and the situation may well be more complicated.

Finally, before leaving hadronic diffraction, we highlight two points about Regge theory whose importance cannot be overemphasized:

- the trajectory function (6) for any given Regge pole depends only on t and is independent of the energy range and the reaction considered; and
- the exchange of two or more Regge poles leads to more complicated terms - *Regge cuts* - which are neglected in most applications, but which must be present at some level of accuracy.

Diffraction in $\gamma^* p$ reactions

The above picture of soft pomeron exchange works quite well for some real photoprocesses like the total photoabsorption cross-section $\sigma_t(\gamma^* p)$ or ρ, ω or ϕ photoproduction. However a steeper rise with energy is observed if s is very large (or x is very small) and an at least moderately hard scale enters the process. More generally, if different data sets are parameterized by a single Regge pole exchange formula, the intercept is found to vary roughly in the range

$$1.08 \leq \alpha_{eff}(0) \leq 1.4 \ .$$

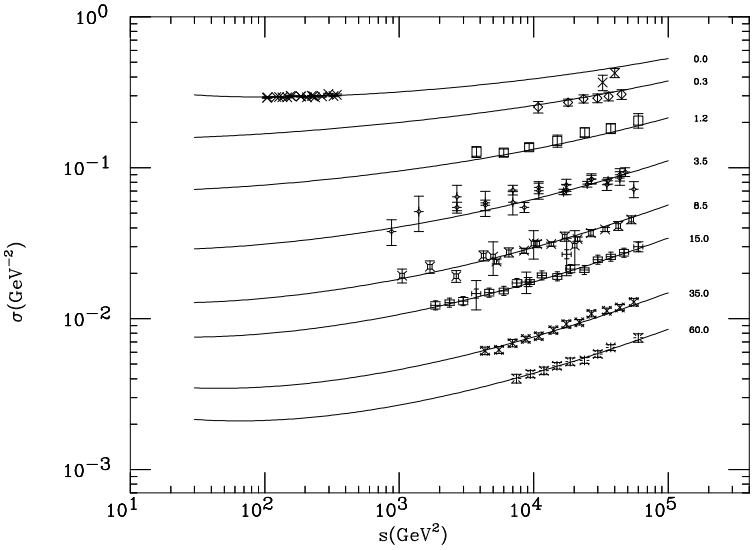

FIGURE 3. Representative sample of data points for the total cross-section $\sigma_{\gamma p}^{tot}$ together with curves calculated from a colour dipole model(see below) (from [13])

The particular value obtained depends on the reaction and on the ranges of Q^2 and x (or equivalently s) considered. This is illustrated in Figure 3, which shows the total cross-section $\sigma_{\gamma p}^{tot}$ as a function of s at various fixed Q^2, where the increase in $\alpha_{eff}(0)$ at high Q^2 and high s, corresponding to low x, is clearly seen.

It follows from the above that diffractive photoprocesses can not be described by a single Regge pole exchange, since this requires a universal energy dependence in all cases. The obvious interpretation is that there is a new phenomenon - "hard diffraction" - which becomes dominant for hard enough scales and large enough energies. If one assumes that this can also be approximated by a Regge pole one is led to the hypothesis of two pomerons: the soft pomeron (8) which dominates in hadronic diffraction and some "soft" photoprocesses; and a second "hard pomeron" which dominates for hard enough scales and large enough energies. This hypothesis has been explored by Donnachie and Landshoff [11] who obtain an excellent fit to data on the proton structure function, the charmed structure function and on J/ψ production (4) for a hard pomeron trajectory

$$\alpha_P(t) \approx 1.42 + 0.10t \ .$$

The varying energy dependence arises from the varying relative importance of the two contributions, which is illustrated in Figure 4 for the proton structure function. Alternatively, Gotsman will discuss [12] a two component model in which the "hard component" is described by a model based on perturbative QCD. In both cases, between the regions of soft and hard diffraction at $Q^2 = 0$ and high Q^2 respectively, there is an extensive transition region in which both can be important.

Hard diffraction and QCD

The discovery of hard diffraction at HERA opens up the subject to perturbative methods in QCD. These can be based on resummations of the perturbative expansion retaining leading terms in $\ln(Q^2/\Lambda^2)$ (DGLAP) or leading terms in $\ln(1/x)$ (BFKL), since both these quantities become large in the relevant kinematic region. The former is the most familiar and has it's best known application in the DGLAP evolution of the structure functions. In particular, it has long been known [14] that this can generate an increasingly steep low-x behaviour as Q^2 increases, and a good fit to the data can be obtained for $Q^2 \geq 1\,\mathrm{GeV}^2$ with the gluon distributions $xg(x, Q^2)$ shown in Figure 5 [15]. The gluon densities at $Q^2 \approx 1\ \mathrm{GeV}^2$ are unstable, implying that the DGLAP picture can not be trusted at such low Q^2 values, but the success at higher Q^2 values is impressive. This "DGLAP picture," based on the dominance of gluon ladder exchanges(see e.g. the talk of Gotsman [12]), can be extended to other diffractive processes at high Q^2, especially for those processes where, in lowest order at least, one can prove factorisation into terms describing the fluctuation of the initial photon into $q\bar{q}$ pairs; the formation of the final particle from the said pairs; and the interaction of the $q\bar{q}$ with the proton [16]. However the gluon distributions required are "skewed" parton distributions [17], which take into account the fact that the incoming and outgoing protons in inelastic processes like (1, 2, 3, 4) have different momenta, even in the forward direction. The empirical study of skewed parton corrections has only just begun [4] [18].

A potential problem with leading, next leading .. $\ln Q^2$ approximations is that as $x \to 0$, neglected terms might become important because although they are lower order in $\ln Q^2$, they are leading order in $\ln(1/x)$. Thus one might expect to see a breakdown of DGLAP at very small-x - but how small? This gives rise to the alternative BFKL approach of leading $\ln(1/x)$ resummation. In leading order this approach predicted the hard pomeron intercept with apparent success, but it runs into serious difficulties beyond leading order. This topic will be discussed by Ross [19] while a succinct comparison of the Regge, BFKL and DGLAP approaches and their relation to each other may be found in the recent review of Ball and Landshoff [20].

In the rest of this talk we will concentrate on two more phenomenological questions:

- Can we find a unified description of both hard and soft diffraction and of the wide variety of diffractive processes?
- When can we expect to see so-called "gluon saturation" effects at small x?

These are conveniently addressed in the context of the *colour dipole model*, to which we immediately turn.

THE COLOUR DIPOLE MODEL

Singly dissociative diffractive γ p processes are conveniently described in the rest frame of the hadron using a picture in which the incoming photon intially dissociates into a $q\bar{q}$ pair a long distance - typically of order of the "coherence length" $1/Mx$ - from the target proton. Assuming that the resulting partonic/hadronic state evolves slowly compared to the size of the proton or nuclear target, it can be regarded as frozen during the interaction. In this approximation, the process will factorize into a probability for the photon to have evolved into a given state $|\alpha>$, times the amplitude for that state to interact with the target. In the colour dipole model, [21,22] the dominant states $|\alpha>$ are assumed to be $q\bar{q}$ states of given transverse size. Specifically

$$|\gamma\rangle = \int \mathrm{d}z\mathrm{d}^2r\ \psi(z,r)|z,r\rangle + \ldots\ , \tag{9}$$

where r is the transverse size of the pair, z is the fraction of light cone energy carried by the quark and $\psi(z,r)$ is the *light cone wave function* of the photon. Assuming that these states are scattering eigenstates (i.e. that z, r remain unchanged in diffractive scattering) the elastic scattering amplitude for $\gamma^* p \to \gamma^* p$ is specified by Figure 6. This leads via the optical theorem to

$$\sigma_{T,L}^{\gamma^* p} = \int \mathrm{d}z\mathrm{d}^2r\ |\psi_\gamma^{T,L}(z,r)|^2 \sigma(s,r,z)\ , \tag{10}$$

for the $\gamma^* p$ total cross-section in deep inelastic scattering, where $\sigma(s,r,z)$ is the total cross-section for scattering dipoles of specified (z,r) from a proton at fixed $s = W^2$. This "dipole cross-section" is a universal quantity for singly-dissociative diffractive processes on a proton target, playing a similarly fundamental role in, for example, open diffraction (1), exclusive vector meson production (3) and (4) and deeply virtual Compton scattering (2).

The dipole cross-section has been evaluated by several groups [23]. Although the assumptions made to do this vary, there are some features in common. The dipole cross-section at a given energy is assumed to be approximately "geometrical", i.e. to depend on the transverse size r of the dipole, but not to depend on z. In addition, approximate QCD behaviour(colour transparency) for small dipoles $r \to 0$ and "hadronic behaviour"
for large dipoles $r \approx$ 1fm are incorporated in varying degrees of detail[1]. A useful summary and comparison of the various approaches may be found in the recent review of McDermott [23]. From now on I shall present results from Forshaw, Kerley and Shaw [13], [24] - [26] who have extracted the dipole cross-section from DIS and real photoabsorption data assuming a form with two terms with a Regge type s dependence:

$$\sigma(s,r) = a_{soft}(r) s^{\lambda_S} + a_{hard}(r) s^{\lambda_H} \tag{11}$$

where the values $\lambda_S \approx 0.08$, $\lambda_H \approx 0.42$ resulting from the fit are characteristic of the soft and hard pomeron respectively. The functions $a_{soft}(r)$, $a_{hard}(r)$ are chosen so that for small dipoles the hard term dominates yielding a behaviour $\sigma \to r^2 (r^2 s)^{\lambda_H}$ as $r \to 0$ in accordance with colour transparency ideas; while for large dipoles $r \approx 1$ fm the soft term dominates with a hadronlike behaviour $\sigma \approx \sigma_0 (r^2 s)^{\lambda_S}$. Correspondingly the photon wavefunction is assumed to be perturbative for small dipoles, with a simple ansatz for confinement effects at large r. The resulting dipole cross-section, determined from DIS and real photoabsorption data, is shown in Figure 7 for various energies in the HERA region.

The above dipole cross-section, determined from DIS and real photoabsorption data, can be used to predict results for other diffractive processes. Successful predictions have been obtained for:

- the charmed structure function [13] by retaining only the charmed quark loop in Figure 6;
- open diffraction (1) from Figure 8, together with an additional contribution from intermediate $q\bar{q}g$ states which is important for large diffractive masses $m_X^2 \gg Q^2$, but small elsewhere [24].
- virtual Compton scattering (2), by replacing the final state photon in Figure 6 by a real photon [26].

The same dipole cross-section can also be used to predict vector meson production reactions like (3, 4), but in this case the vector meson wavefunctions are also required.

Saturation

The dipole model is particularly useful for discussing saturation effects, since it incorporates both soft and hard diffraction, associated with small and large dipoles respectively. There are actually two types of saturation effect, which are quite distinct and should not be confused.

Low Q^2 saturation. As can be seen in Figure 7, the dipole cross-section increases rapidly as a function of the dipole size r at small r, but then "saturates" to a slowly varying cross-section of hadronic size at larger r values. This change - and the fact that it shifts to smaller r as s increases -is crucial to describe the form of the change from approximate scaling to the observed $Q^2 \to 0$ (and hence $x \to 0$) behaviour at fixed s. To see this we note that the Q^2 dependence in (10) arises entirely from the wavefunction. As Q^2 decreases, larger r values are explored and the slowly varying dipole cross-section results in a weakening Q^2 dependence for $\sigma_{\gamma^* p}$. When $Q^2 \ll 4m_q^2$, where m_q is the constituent quark mass, the wavefunction and $\sigma_{\gamma^* p}$ become independent of Q^2 so that $F_2 \propto Q^2$ as $Q^2 \to 0$ as required.

Gluon saturation. For high enough energies, the assumed s^λ ($\lambda > 0$) behaviours assumed above must be tamed by unitarity effects, especially for the hard term with $\lambda_H \approx 0.4$. At fixed Q^2, $x \to 0$ as $s \to \infty$ and the resulting softening of the corresponding $x^{-\lambda_H}$ behaviour is associated with gluon saturation in the quark-parton language. Gluon saturation can be incorporated into dipole and other closely related models by hand [27,28] or using the eikonal approximation [30,31] but are not included in (11). Hence the fact that an excellent fit is obtained to the DIS data using (11) means that the current HERA data are not at sufficiently high s to *require* the saturation effects that are built into some other dipole models [27,28]. We note that our model agrees with the standard Caldwell plot Figure 9, where the turn over as x decreases occurs because Q^2 is also decreasing and is understood as a low

Q^2 saturation effect. No such effect is predicted in our model if x is decreased at fixed Q^2, as confirmed by the preliminary ZEUS97 data [32].

A strong indication of when saturation effects will be needed is given in Figure 7. As can be seen, the cross-section for small dipoles is initially small but increases rapidly and at the top of the accessable HERA range is becoming commensurate with the slowly increasing "hadronic" behaviour af the large dipoles. It is at this point that saturation effects are expected to become important; if they don't, the cross-section for small dipoles will exceed that for large dipoles at higher energies and the dipole cross-section will paradoxically decrease with increasing size r. Saturation effects are therefore expected to play an important role just beyond beyond the HERA range, in the planned THERA region with $s_{max} \approx 10^6$ GeV^2.

REFERENCES

1. M. Arneodo, "Diffraction at HERA - an Introduction," Proceedings of Photon97.
2. see for example the review of A. Hebecker, Phys. Rep. **331** (2000) 1 and references therein.
3. See the talks by H. Mahlke-Krueger and by C. Johnson, these proceedings.
4. See the talk by R. Stamen, these proceedings.
5. See the talks by S.Kananov and by A.Savin, these proceedings.
6. See the talk by K. Klimek, these proceedings.
7. See the talks by A. Wyatt and by B. List, these proceedings.
8. See the talks by M. Wadhwa, M.Przybycien, N.Zimin and M.Kienzle, these proceedings.
9. N. Cartiglia, "Diffraction at HERA" lanl hep-ph/9703245.
10. A.Donnachie and P.V.Landshoff, Phys.Lett. **B296** (1992) 139.
11. A.Donnachie and P.V.Landshoff, Phys.Lett. **B437** (1998) 408.
12. See the talk by E. Gotsman, these proceedings.
13. J.R. Forshaw, G. Kerley and G. Shaw, Phys. Rev. **D60** (1999) 074012.
14. A. De Rujula et al, Phys. Rev.**D10** (1974) 1649.
15. ZEUS collaboration, Eur.Phys.J. **C7** (1999) 609
16. J.C. Collins, L. Frankfurt and M. Strikman, Phys. Rev. **D56** (1997) 2982; J.C. Collina and A. Freund, Phys.Rev. **D59** (1999) 074009
17. For a recent review, see Zhang Chen hep-ph/0008015.
18. L. Frankfurt, A. Freund and M. Strikman, Phys.Rev. **D58** (1998) 114001; erratum **D59** (1999) 119901.
19. D.A. Ross, these proceedings. See also G.Salam, lanl hep-ph/0005304
20. R.D. Ball and P.V. Landshoff J.Phys. **G26** (2000) 672-682 hep-ph/9912445.
21. N.N. Nikolaev and B.G. Zakharov, Z. Phys. **C49** (1991) 607; Z. Phys. **C53** (1992) 331
22. A. H. Mueller, Nucl. Phys. **B415** (1994) 373; A. H. Mueller and B. Patel, Nucl. Phys. **B425** (1994) 471
23. See the review of M.F.McDermott DESY report 00-126, hep-ph/0009086 and references therein.
24. J.R. Forshaw, G. Kerley and G. Shaw, Nucl.Phys. A675 (2000) 80; hep-ph/9910251.
25. J.R. Forshaw, G. Kerley and G. Shaw, Proc. of DIS2000, to be published. hep-ph/0009235.
26. J.R. Forshaw, R. Sandapen and G. Shaw, to be published.
27. K. Golec-Biernat and M. Wüsthoff, Phys. Rev. **D59** (1999) 014017, **D60** (1999) 114023.
28. M. McDermott, L. Frankfurt, V. Guzey and M. Strikman, hep/ph9912547v2.
29. E. Gotsman, E. Levin and U. Maor, Phys. Lett. **B425** (1998) 369; Eur. Phys. J **C5** (1998) 303.
30. E. Gotsman, E. Levin, U. Maor and E.Naftali Nucl.Phys. **B539** (1999) 535; Eur. Phys. J **C10** (1999) 689.
31. A. Capella, E.G. Ferreiro, C.A. Selgado and A.B. Kaidalov. hep-ph/0006233.
32. R. Yoshida; talk for the ZEUS collaboration at DIS99. Nucl. Phys. **B79** (1999) 83.

[1)] Very large dipoles $r \gg$ 1fm make a negligible contribution, since the wavefunction factor in (10) decreases exponentially at large r.

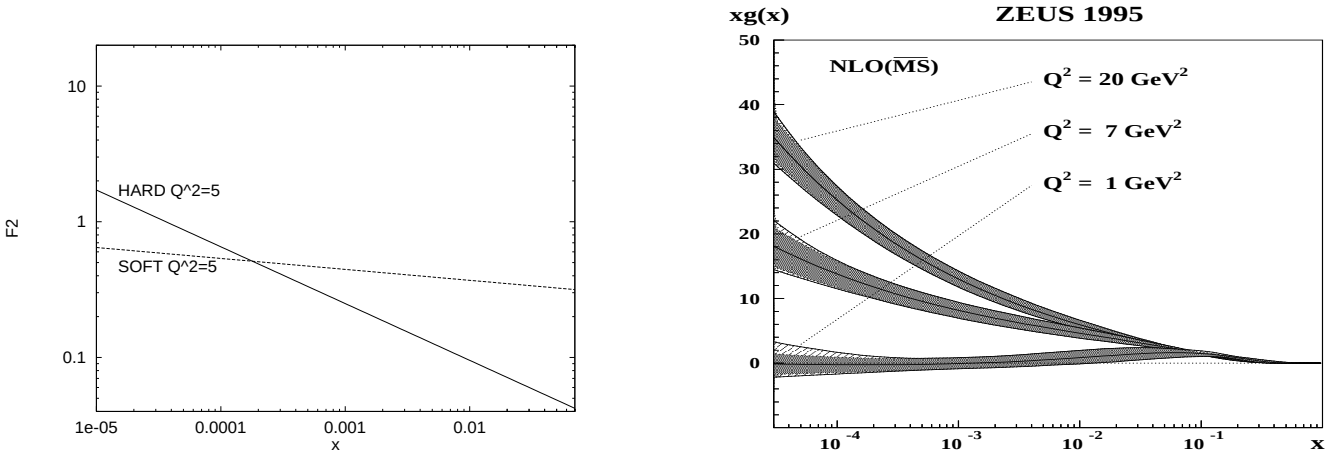

FIGURE 4. Above left: relative magnitudes of hard and soft pomeron contributions at $Q^2 = 5$. As Q^2 increases the range of hard pomeron dominance extends to larger x. (Figure from [11])

FIGURE 5. Above right: the gluon density $xg(x, Q^2)$ extracted from next leading order fits to the ZEUS $F_2(x, Q^2)$ data. (Figure from [15])

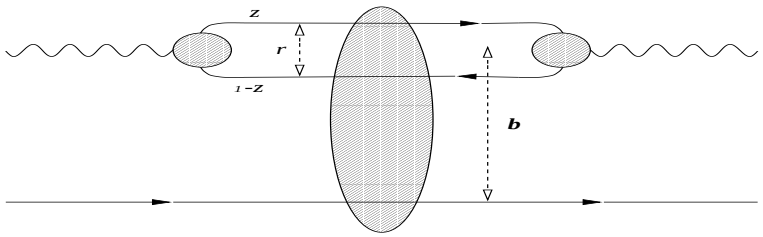

FIGURE 6. The colour dipole model for $\gamma^* p \to \gamma^* p$.

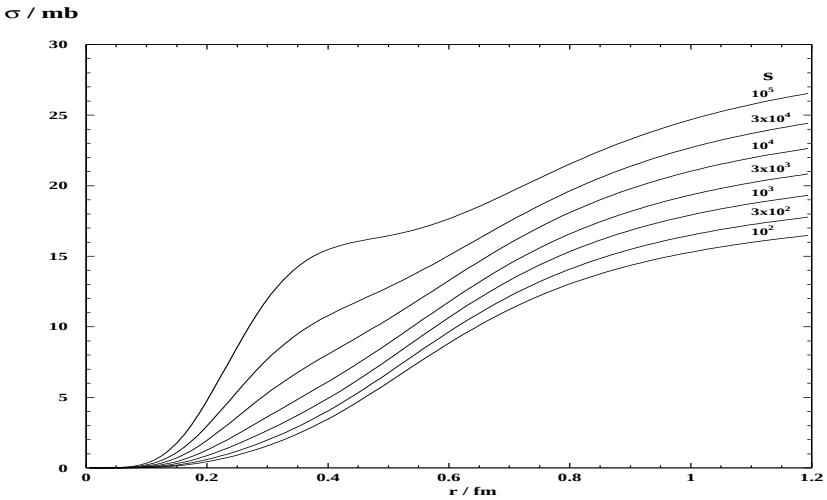

FIGURE 7. The dipole cross-section as a function of s in the HERA range.

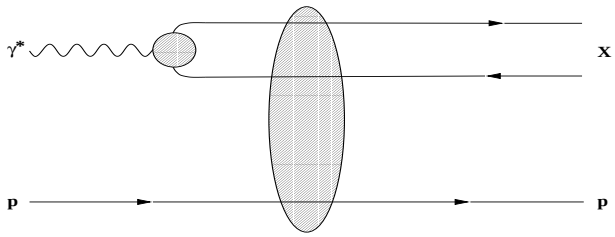

FIGURE 8. The dipole contribution to open diffraction (1).Figure from [25].

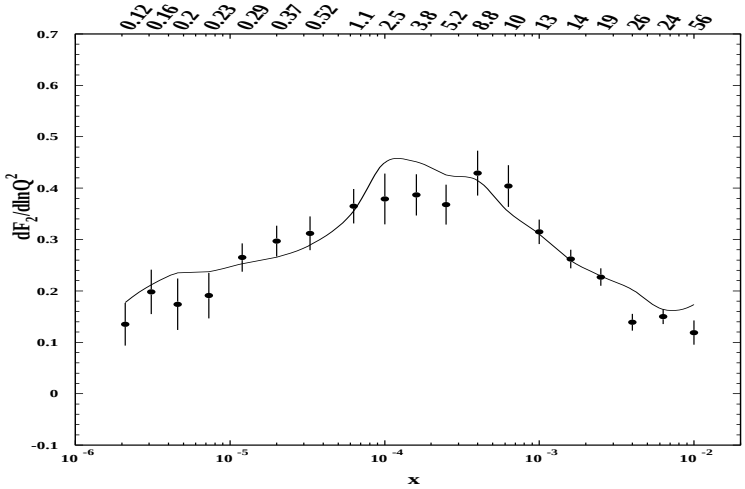

FIGURE 9. The Caldwell plot. Predictions are made at the Q^2 values of the data points and roughly interpolated. (Figure from [25])